

University of Montana

## ScholarWorks at University of Montana

---

Water Topos: A 3-D Trend Surface Approach to  
Viewing and Teaching Aqueous Equilibrium  
Chemistry

Open Educational Resources (OER)

---

12-2021

### Chapter 3.1: Visualization of the Nernst Equation Via 3-D Topo Surfaces: $E^0$ Plateaus, Left-Hand Bluffs, Front Cliffs and Reaction Paths

Garon C. Smith  
*University of Montana, Missoula*

Md Mainul Hossain  
*North South University, Bangladesh*

Follow this and additional works at: <https://scholarworks.umt.edu/topos>

 Part of the [Chemistry Commons](#)

Let us know how access to this document benefits you.

---

#### Recommended Citation

Smith, Garon C. and Hossain, Md Mainul, "Chapter 3.1: Visualization of the Nernst Equation Via 3-D Topo Surfaces:  $E^0$  Plateaus, Left-Hand Bluffs, Front Cliffs and Reaction Paths" (2021). *Water Topos: A 3-D Trend Surface Approach to Viewing and Teaching Aqueous Equilibrium Chemistry*. 8.  
<https://scholarworks.umt.edu/topos/8>

This Book is brought to you for free and open access by the Open Educational Resources (OER) at ScholarWorks at University of Montana. It has been accepted for inclusion in Water Topos: A 3-D Trend Surface Approach to Viewing and Teaching Aqueous Equilibrium Chemistry by an authorized administrator of ScholarWorks at University of Montana. For more information, please contact [scholarworks@mso.umt.edu](mailto:scholarworks@mso.umt.edu).

## Chapter 3.1

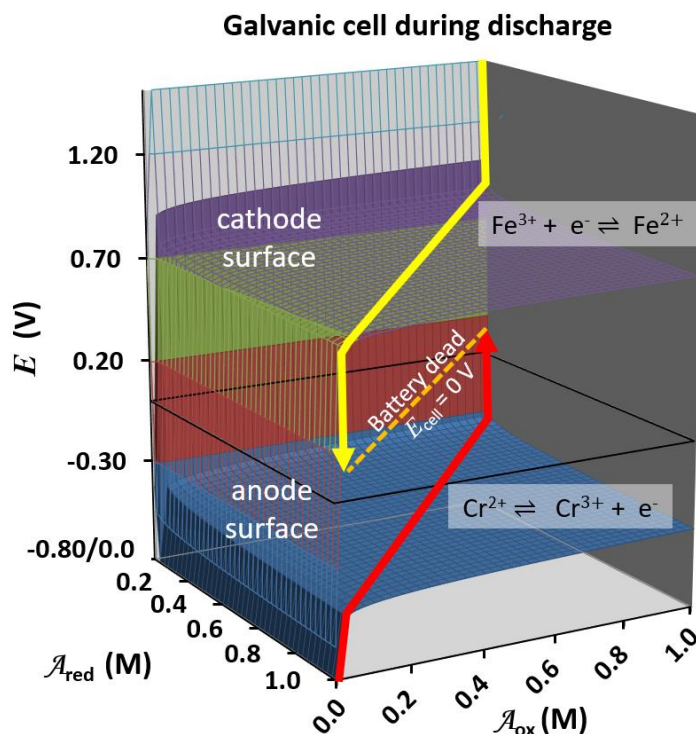
# Visualization of the Nernst Equation Via 3-D Topo Surfaces: $E^0$ Plateaus, Left-Hand Bluffs, Front Cliffs and Reaction Paths

Garon C. Smith<sup>1</sup> and Md Mainul Hossain<sup>2</sup>

<sup>1</sup>Department of Chemistry and Biochemistry, University of Montana, Missoula, MT 59812, USA <sup>2</sup>Department of Biochemistry and Microbiology, North South University, Dhaka 1229, Bangladesh

### Abstract

A new 3-D graphical representation of oxidation–reduction (redox) processes in aqueous solutions has been developed utilizing a composition grid for which the  $x$ -axis carries the activity of the reduced form of the redox couple and the  $y$ -axis carries the activity of the oxidized form. The Nernst equation potential corresponding to the redox couple's activities at each grid point is plotted above it as a  $z$ -coordinate. This creates a 3-D trend surface (a topo) over the grid. The topos typically have a steep left-hand bluff and a precipitous front cliff that are encountered when one or the other of the redox couple species is near depletion. In between these two features, much of the topo is a broad plateau with an elevation near the  $E^0$  for the half-reaction. Discharge paths during the operation of a galvanic cell appear as oppositely-trending, angled paths across a pair of vertically separated surfaces. The cell dies when the two reaction paths achieve the same potential, *i.e.*, identical  $z$ -coordinates. Redox TOPOS, a free downloadable Microsoft Excel workbook, generates 1681-point (41 x 41) 3-D topos once a redox couple has been identified and all Nernst equation parameters have been entered. Also included a supplementary files are a set of PowerPoint lecture slides and a document “Teaching with Redox TOPOS” containing sections for use in lecture and exercises for homework or discussion for introductory college courses and third-year or graduate physical chemistry, analytical chemistry, biochemistry, and geochemistry courses.



### 3.1.1 Introduction

The two most fundamental types of chemical reactions are oxidation-reduction (*i.e.*, redox) and acid-base. Redox reactions involve the transfer of electrons; acid-base reactions encompass the transfer of protons. Of the two, redox is broader in scope because almost any atom can become engaged in electron transfer. But because protons are buried deep in the nucleus, only a hydrogen ion is bare enough to be available as a proton transfer. Most introductory and analytical chemistry courses apply the Nernst equation to calculate potentials in redox problems. But many subtle aspects of aqueous redox equilibria are missed by simply looking at the calculated results for a single set of solution conditions, or even a redox titration. Take, for example, the difference between calculating the potential for a single solution composition versus the series of potentials that are encountered in working electrochemical cells, *e.g.*, discharging a battery. This chapter offers a graphical method to track the redox chemistry as galvanic cells operate. A redox composition grid is employed that incorporates a wide range of activities (*i.e.*, concentrations adjusted for ionic strength) for both the oxidized and reduced forms of a redox couple. When the Nernst potential is plotted above this composition grid, three-dimensional surfaces emerge showing trends in half-cell potentials as calculated

by the Nernst equation. Tracks across the trend surfaces indicate half-reaction performance as the cell runs. The free, downloadable Excel workbook Redox TOPOS gives a nice visual meaning to what  $E^0$  represents and where the thermodynamics of an electrochemical cell indicate that it is “dead”. It also allows the user to see how varying each parameter in the Nernst equation affects the trend surface’s appearance. Our Nernst topo surfaces are subsequently used in Chapter 3.2 to more completely illustrate why batteries deliver a fairly constant voltage until they suddenly die.

The Redox TOPOS software will be useful for introductory chemistry course students to explore how the Nernst equation behaves as different parameter values in it are changed. “Slider” controls on the main spreadsheet allow almost instantaneous recalculation of the entire trend surface as a variable is manipulated –  $E^0$ , temperature, the number of electrons. Changeable input parameters also include stoichiometries, pH, and  $\text{H}_3\text{O}^+$  or  $\text{OH}^-$  species. Understanding the detailed discussion of reaction tracks and the interactions between the surfaces for a pair of half-reactions, however, will be more appropriate for upper division or graduate courses in analytical chemistry, physical chemistry, biochemistry and geochemistry. The free software could also be helpful to researchers who are interested in predicting redox properties in natural waters, for example, anticipating events leading to the onset of a harmful algal bloom (HAB).<sup>1,2</sup> Also included as additional downloadable files are: 1) a PowerPoint lecture about the use and interpretation of the Redox TOPOS program; and 2) teaching materials with learning goals and sample exercise suggestions for instructors who wish to employ the Redox TOPOS program in their courses.

### 3.1.2 The Nernst Equation and the Redox Composition Grid

The Nernst equation (eq 3.1-1) is typically presented as:

$$E = E^0 + \frac{RT}{nF} \ln \frac{\mathcal{A}_{\text{ox}}^a}{\mathcal{A}_{\text{red}}^b} \quad (3.1-1)$$

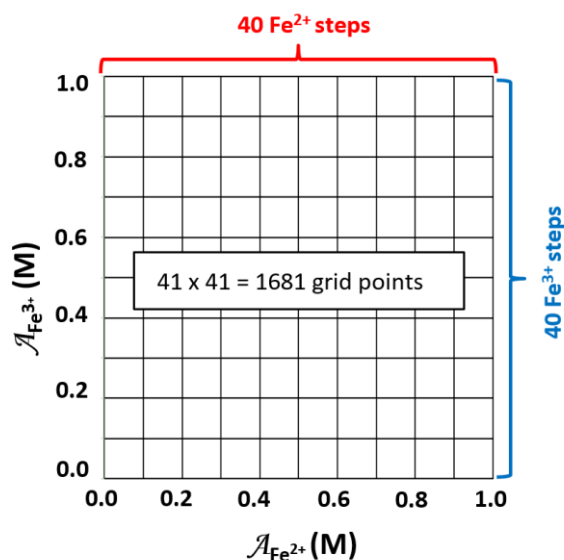
where  $E$  is the potential expressed in volts,  $E^0$  is the standard reduction potential for unit activities at 298K,  $R$  is the universal gas constant,  $T$  is temperature in kelvin,  $n$  is the number of electrons transferred in the reaction,  $F$  is the Faraday

constant, the  $\mathcal{A}$ s represent the activities of the oxidized and reduced forms of the half-reaction species, and  $a$  and  $b$  are coefficients from the half-reaction. V.A. Shaposhnik<sup>3</sup> traces the role that Nernst played in developing the form of the equation that appears in most textbooks. Helmholtz, Nernst's mentor, derived an equation in 1877 for a Galvanic concentration cell – one in which both electrodes are identical and the electrolytes in the two half-cells differ only in concentration. In 1889, Nernst published a formula in which he replaced an empirical factor in the Helmholtz equation with one containing the familiar  $R$ ,  $T$ ,  $n$  and  $F$  parameters.<sup>4</sup> The equation conventionally called “the Nernst equation” first appeared in an 1898 paper by Rudolf Peters.<sup>5</sup> Peters and Nernst both worked for Ostwald at Leipzig University. The Peters equation is applicable not only to concentration cells, but also to cells in which the two half-reactions are completely distinct from one another.

Use of a redox composition grid helps visualize the overall behavior of the Nernst equation, especially during electrochemical cell operation. The redox composition grid differs from the titration-dilution grids that were employed in earlier chapters in this book. For the redox grid employed here, the two axes hold the activities of both the oxidized and reduced forms of the substance comprising the redox couple. Figure 3.1-1, for example, displays the redox composition grid for the half-reaction involving the transfer of a single electron between  $\text{Fe}^{3+}$  and  $\text{Fe}^{2+}$  (eq 3.1-2):



**Figure 3.1-1.** The redox composition grid for the  $\text{Fe}^{3+} + e^- \rightleftharpoons \text{Fe}^{2+}$  redox couple.



Any single calculation involving the Nernst equation corresponds to substituting in a specific  $(x, y)$  pair of coordinates from the grid. The  $x$ -coordinate signifies the activity of the reduced form ( $\mathcal{A}_{\text{Fe}^{2+}}$ ) and the  $y$ -coordinate signifies the activity of the oxidized form ( $\mathcal{A}_{\text{Fe}^{3+}}$ ). As implemented in Redox TOPOS, there are 40 grid increments in either direction resulting in a total of 41 x 41 or 1,681 grid points in a trend surface. The origin is always at (0.0,0.0) but the upper value is adjustable. As downloaded, the default upper value is 1.00 M on each axis.

### 3.1.3 The Nernst Equation Surface for a Single Redox Half-Reaction

Substituting every grid pair of  $(\mathcal{A}_{\text{Fe}^{2+}}, \mathcal{A}_{\text{Fe}^{3+}})$  into the Nernst equation generates the third value needed as a  $z$ -coordinate to construct the  $\text{Fe}^{3+}/\text{Fe}^{2+}$  topo surface plot. Two versions of the redox grid are possible – one in which the  $x$ - and  $y$ -axes are linear (Figure 3.1-2a) and an alternate version in which the  $x$ - and  $y$ -axes are logarithmic (Figure 3.1-2b). Each has its merits.

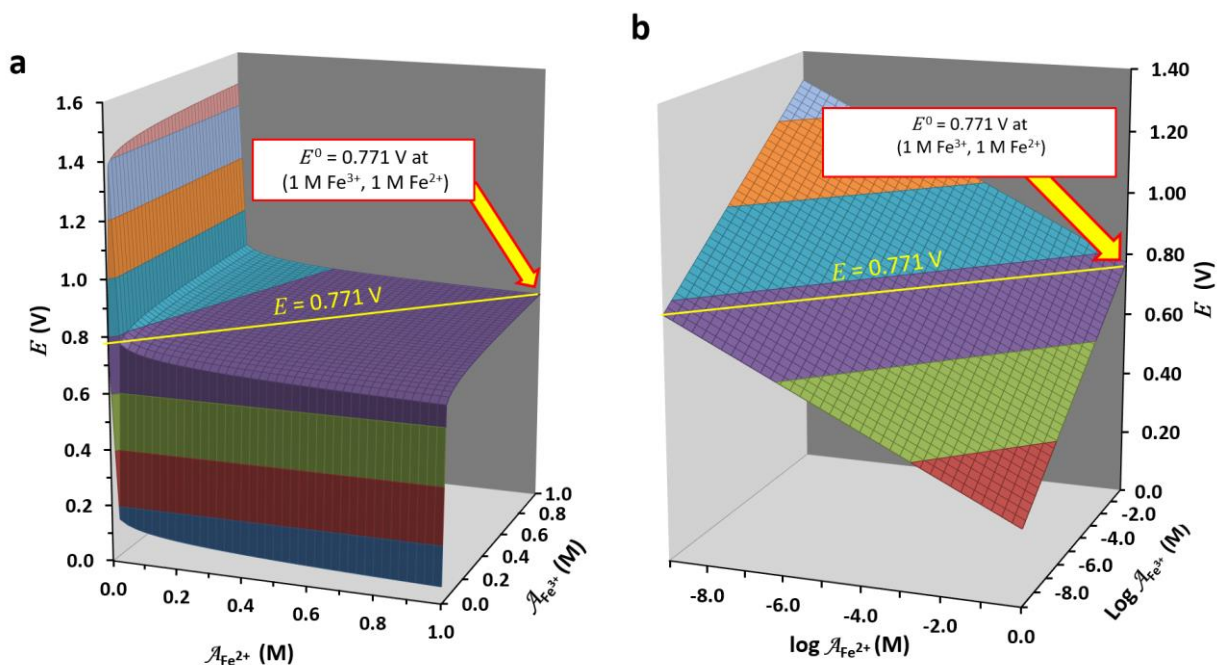


**Figure 3.1-2.** The Nernst surface for the  $\text{Fe}^{3+} + \text{e}^- \rightleftharpoons \text{Fe}^{2+}$  redox couple. a) linear axes; b) logarithmic axes.  $E^0$  values used here and in other plots are from Reference 6.

The linear topo looks like a chair with a twist while the logarithmic topo is an inclined plane. The linear plot of Panel a illustrates that the potential for a redox couple never moves far from the  $E^0$  value over most grid points. We call this broad flat area the “ $E^0$  plateau”. The definition of  $E^0$  itself is associated with the grid point at the right-hand back corner of Figure 3.1-2a at (1.0,1.0) and the corresponding grid point on the logarithmic composition grid of Figure 3.1-2b at (0.0,0.0). For the  $E^0$  on both surfaces, the  $\mathcal{A}_{\text{Fe}^{2+}}$  and  $\mathcal{A}_{\text{Fe}^{3+}}$  are at unit activity. This broad plateau region on the linear topo constitutes the basis behind redox buffering.<sup>7</sup> (Any flat spot on a composition grid surface indicates a buffer situation of one sort or another.) Thus, the Nernst equation basically says that  $E^0$  is the “standard potential term” for a half-cell’s voltage under most conditions (Figure 3.1-3). The second term in the equation adjusts for fluctuations in temperature, the number of electrons and the ratio of the oxidized and reduced forms, especially when one or the other redox couple species is approaching very small values. Once close to either axis, the change in potential is dramatic, leading to the left-hand bluffs and front cliffs. In fact, we have artificially truncated the surfaces along both axes by using an activity of  $1.0 \times 10^{-24}$  M instead of 0. At activities of 0, the surface would rise to  $+\infty$  along the  $y$ -axis and drop to  $-\infty$  along the  $x$ -axis.

**Figure 3.1-3.** The two contributing terms of the Nernst equation.

$$E = E^0 + \frac{RT}{nF} \ln \frac{\mathcal{A}_{\text{ox}}^a}{\mathcal{A}_{\text{red}}^b}$$

As mentioned above, the linear axis topo is mostly a plateau at the level of  $E^0$ . This is 0.771 V for the  $\text{Fe}^{3+}/\text{Fe}^{2+}$  example. A detailed examination of the plateau reveals that, for a 1:1 stoichiometry between the redox couple’s forms, equipotential lines radiate outward from the origin like spokes on a wheel. The line between the origin and the  $E^0$  grid point at (1.0,1.0) is the locus of points for which  $\mathcal{A}_{\text{Fe}^{2+}} = \mathcal{A}_{\text{Fe}^{3+}}$ . For this collection of points, the ratio of  $\mathcal{A}_{\text{Fe}^{3+}}/\mathcal{A}_{\text{Fe}^{2+}}$  is always 1.0 and the adjustment term of the Nernst equation goes to zero. Along this line, the  $E$  of the half-cell is equal to the  $E^0$  for the half-cell. Points to the right of that line are slightly lower than  $E^0$ ; points to the left are slightly higher.

Equipotential lines on the top surfaces are linear whenever there is a 1:1 ratio between the oxidized and reduced forms of a redox couple. The  $E = E^0$  line of Figure 3.1-2a is an example of this. For half-reactions where the stoichiometry between the redox couple species is not 1:1, the locus of equipotential points will be along a path that preserves a constant ratio,  $Q$ , between the oxidized and reduced forms, *i.e.*,

$$Q = \frac{\mathcal{A}_{ox}^a}{\mathcal{A}_{red}^b} \quad (3.1-3)$$

Rearranging this into an equation that permits tracking across the redox composition grid gives

$$\mathcal{A}_{ox} = \left(Q \mathcal{A}_{red}^b\right)^{\frac{1}{a}} \quad (3.1-4)$$

The Redox TOPOS software provides a composition grid plot showing the shape of isopotential lines computed from the stoichiometry that has been entered. Figure 3.1-4 illustrates these plots for oxidized form/reduced form stoichiometries of 1:1 (Panel a) and 2:1 (Panel b).

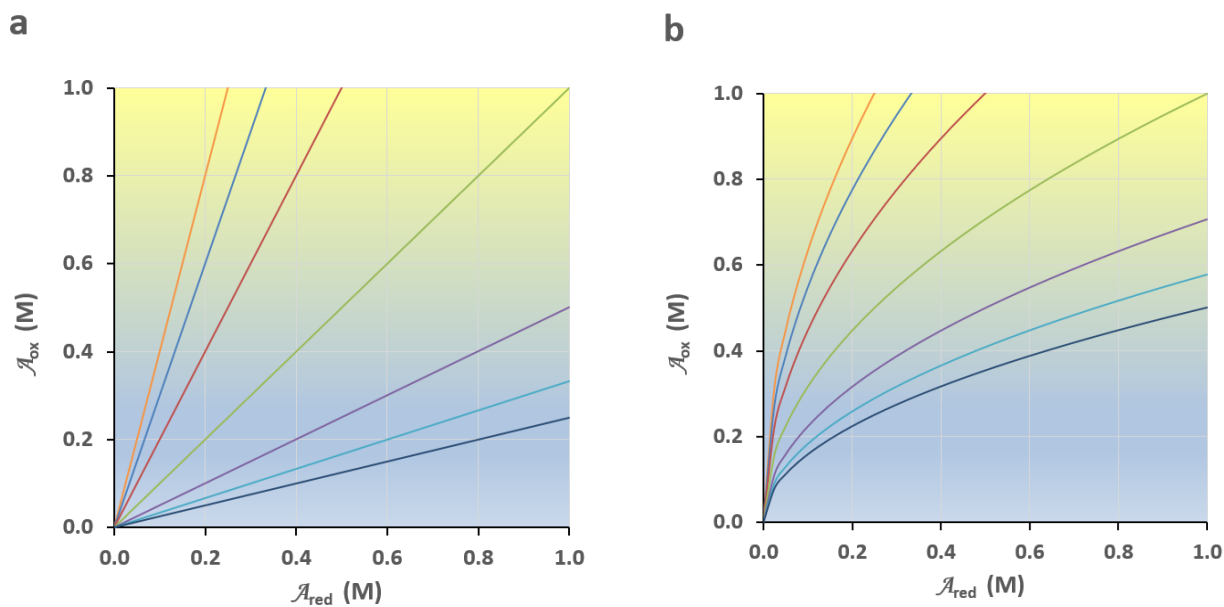


**Figure 3.1-4.** Isopotential line shapes on the linear composition grid for two oxidized form/reduced form stoichiometries. a) 1:1; b) 2:1

The logarithmic trend surface is not quite as rich in new insights, but it does demonstrate that potentials are directly proportional to log activities over many

orders of magnitude. This is important for the design and operation of ion selective electrodes. The distribution of grid points for the log topo is quite different than in the linear topo. Because the log axes expand the low end of the scales, most grid-points on the logarithmic axis surface are within the first row of grid cells on the linear surface. With the exception of the  $E^0$  point, the remainder of the log surface grid points already represent situations in which at least one form of the redox couple is near depletion. Thus, the potentials vary more quickly as one moves away from the  $E^0$  value. Isopotential lines on the log surface are always straight, but may run across the grid at different angles. For a 1:1 case, the lines are parallel to the grid diagonal. For other stoichiometries, they are not.

The linear Nernst equation topo looks largely the same no matter what range of activities is employed. The axes for the redox composition grid of Figure 3.1-2a extend to activities of 1.0 M, a large value compared to those found in most real solutions. The upper limit of 1.0 M was used expressly to illustrate the grid-point that defines the  $E^0$  conditions. Restriction of the activity range on the linear axes to a maximum value of 0.10 M or even 0.010 M makes an almost imperceptible difference in the appearance of the Nernst surface (Figure 3.1-5).

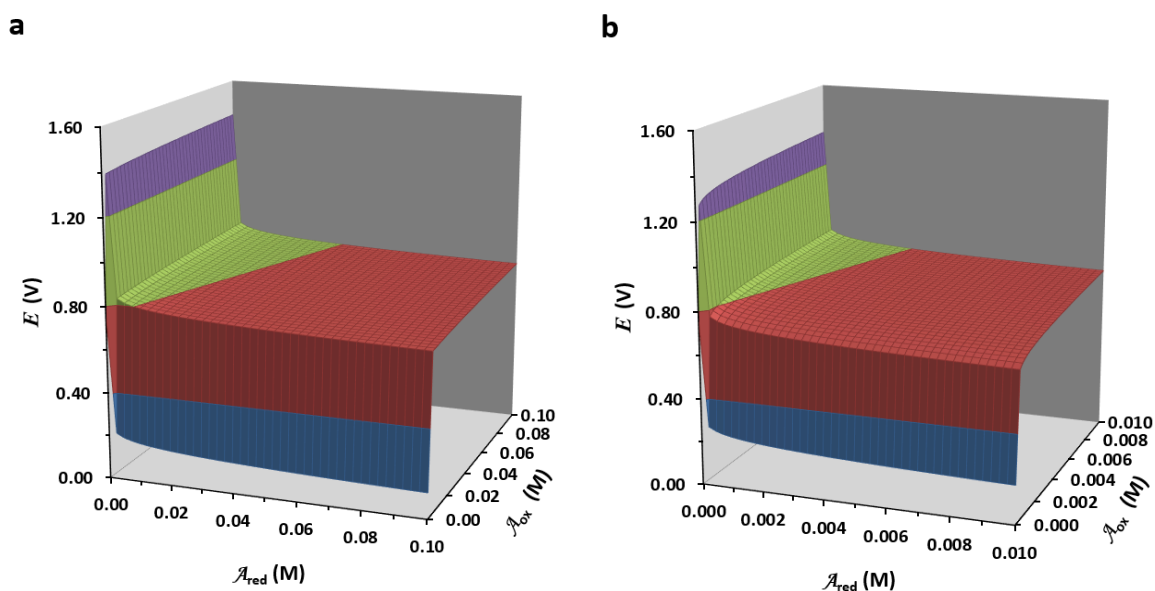


**Figure 3.1-5.** The Nernst surface of the  $\text{Fe}^{3+} + e^- \rightleftharpoons \text{Fe}^{2+}$  redox couple for more dilute systems. a) 0.10 M maximum activity; b) 0.010M maximum activity.

The only differences in the more dilute topos reside in the left-hand bluff and the front cliff. These differences are mostly an artifact of maintaining an activity of  $1.0 \times 10^{-24}$  M to avoid zeroes in the adjustment term's log ratio. All other grid points retain the same  $\mathcal{A}_{\text{Fe}^{3+}}/\mathcal{A}_{\text{Fe}^{2+}}$  ratio, so the corresponding adjustment term values are identical assuming ionic strength is maintained at a constant background level. The principal plateaus off both panels sit at an elevation centered on  $E = E^0 = 0.771\text{V}$ . A change that makes no visual difference here, however, is the capacity of the system to respond to  $e^-$  fluxes. This point will be discussed further in the next section which addresses reaction paths on Nernst surfaces.

### 3.1.4 Discharge Reaction Paths

The richness of insights provided by viewing the Nernst topo surfaces emerges when potentials for the series of points corresponding to the operation of an electrochemical cell are tracked across the grid. This section defines reaction paths for redox processes. Reaction paths are employed in subsequent sections to illustrate galvanic and concentration cell discharges. The reaction paths superimposed on topo pairs provide a visual depiction of an electrochemical cell's equilibrium point, *i.e.*, where it dies, and a method for determining which cell reaction direction is spontaneous.

Given the manner in which the linear redox composition grids are constructed, the progress of any half-reaction that occurs will generate a slanted line across the grid with a negative slope. As oriented here, reduction half-reactions will proceed downward and to the right; oxidation half-reactions will proceed upward and to the left. For a half-reaction in which a single electron is transferred, the slope of the line will always be  $-1.0$ , *i.e.*, a  $45^\circ$  diagonal across the grid. This is a result of the half-reaction's stoichiometry. Consider the  $\text{Fe}^{3+}/\text{Fe}^{2+}$  half-cell proceeding as a reduction reaction (a repeat of eq 3.1-2) with the relative changes that occur upon a discharge reaction underneath it in colored fonts:



For each  $\text{Fe}^{3+}$  that disappears in a reduction process, an  $e^-$  is consumed and a corresponding  $\text{Fe}^{2+}$  appears.

Figure 3.1-6 depicts the reaction path for the potentials encountered as a reduction half-cell containing  $\text{Fe}^{3+}$  and no  $\text{Fe}^{2+}$  participates in a redox reaction. The starting point is located where the activity of  $\text{Fe}^{3+}$  is 1.0 M and the activity of  $\text{Fe}^{2+}$  is  $1.0 \times 10^{-24}$  M. Recall that this is what we used to indicate essentially no  $\text{Fe}^{2+}$  is available. We use it in place of "0" which would give a  $+\infty$  value for  $E$ . The path shown represents a discharge reaction until half of the  $\text{Fe}^{3+}$  has been converted to  $\text{Fe}^{2+}$ , *i.e.*, both species are now at an activity of 0.5 M. On the linear composition grid, the reaction path is a diagonal line that runs from the upper left to the grid's center. Notice that the path descends the left-hand bluff very rapidly before proceeding to the center of the  $E^0$  plateau (Figure 3.1-6a). By the time the reaction has moved to only its second grid point at (0.025, 0.975), the potential is already nearing the  $E^0$  value. (NOTE: Figure 3.1-6b only shows every fourth grid interval.) When the path reaches its final point, where  $\mathcal{A}_{\text{Fe}^{3+}} = \mathcal{A}_{\text{Fe}^{2+}}$ , the half-cell potential will be sitting at the same voltage as  $E^0$ .

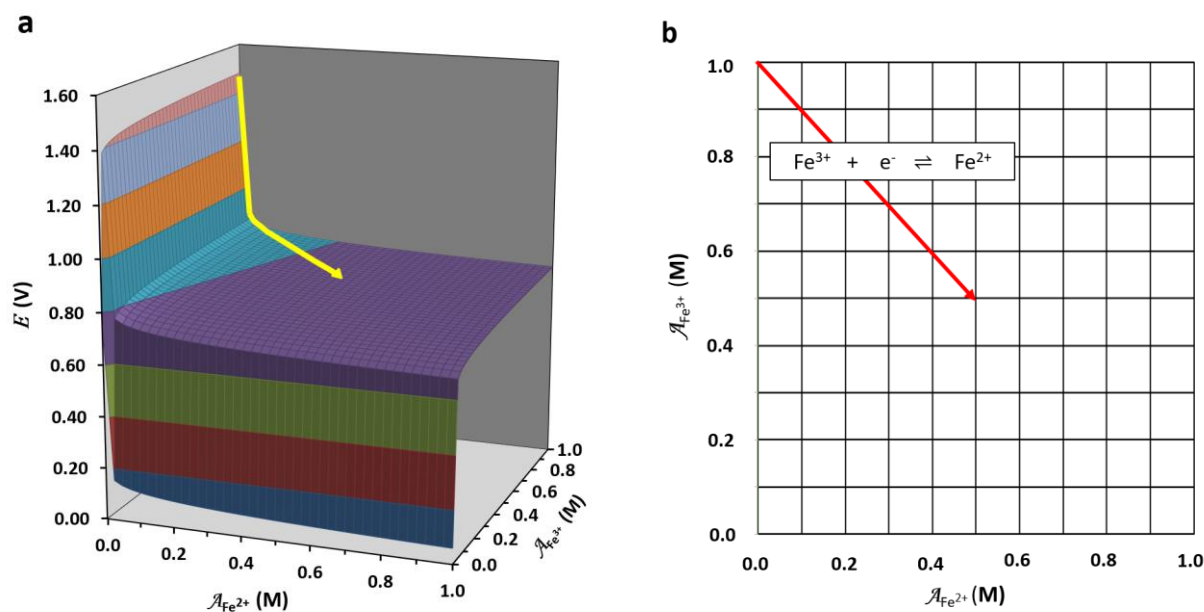
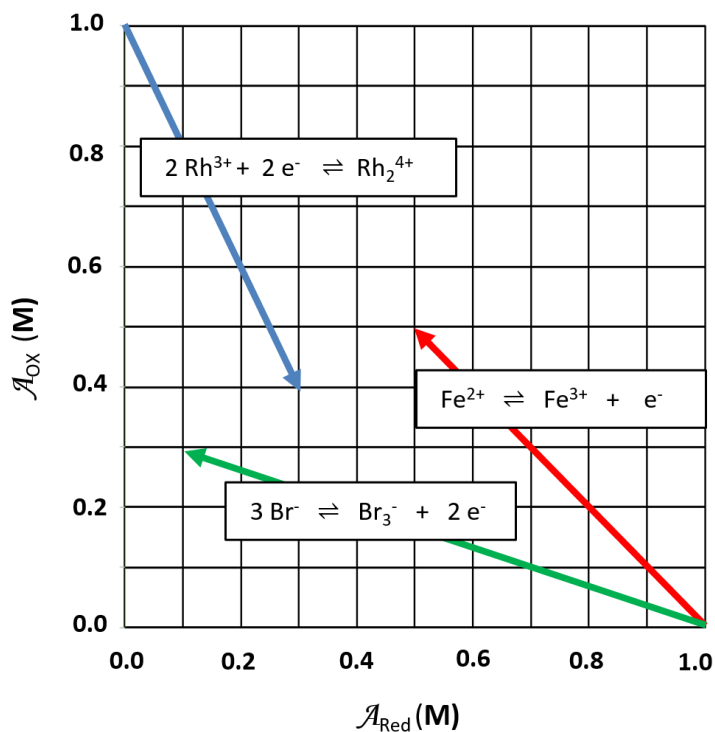


**Figure 3.1-6.** The discharge reaction path for the  $\text{Fe}^{3+}/\text{Fe}^{2+}$  redox couple as the activity of  $\text{Fe}^{3+}$  goes from 1.0 to 0.5 M in the half-cell. a) topo; b) composition grid.

Half-reactions for redox couples where there are unequal stoichiometric ratios between the oxidized and reduced forms will have reaction paths that run at angles other than  $45^\circ$ . Figure 3.1-7 illustrates several additional reaction paths to give a sense for these situations. The rhodium reduction reaction path runs at a slope of -2.0 to the right and down because for each 2  $\text{Rh}^{3+}$  that react, there is only one  $\text{Rh}_2^{4+}$  ion that appears. Two different oxidation paths are shown. The oxidation of  $\text{Fe}^{2+}$  to  $\text{Fe}^{3+}$  has a 1:1 stoichiometry and a slope of -1 that runs up and to the left. That for the bromine half-reaction has a slope of -0.33 running upward and to the left. It takes three bromide ions,  $\text{Br}^-$ , to produce a single tribromide ion,  $\text{Br}_3^-$ .

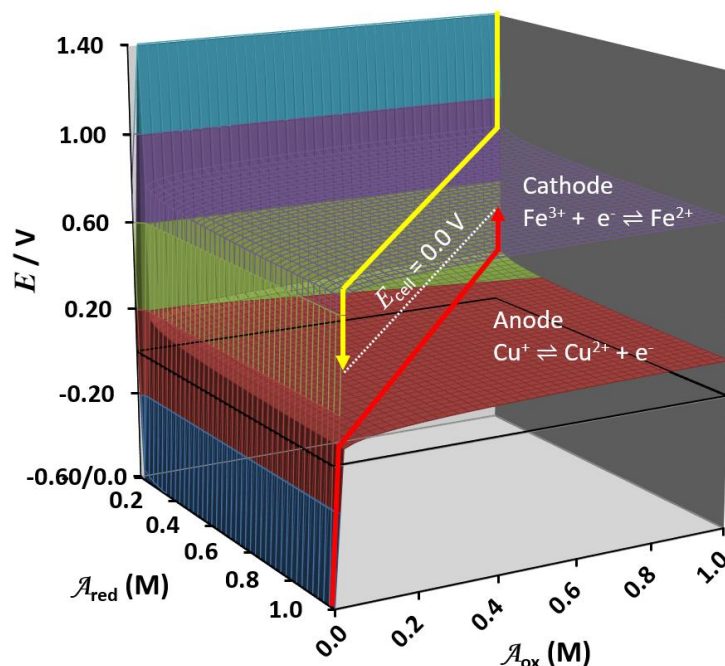
**Figure 3.1-7.** Reaction paths for three redox couples, two of which have unequal coefficients in their half-reactions. One is a reduction reaction (blue) and two are oxidation reactions (green and red).



### 3.1.5 Galvanic Cell Topos

A typical galvanic cell involves two half-reactions, one for each half-cell, so two Nernst surfaces are needed to display the sequence of potentials that occur as the cell operates. For purposes of illustration, consider a galvanic cell in which  $\text{Fe}^{3+}$  at unit activity in one half-cell oxidizes  $\text{Cu}^+$  at unit activity in the other half cell (Figure 3.1-8). Assume here that the other half of each redox couple is essentially not present (*i.e.*,  $1.0 \times 10^{-24}$  M for the truncation limits).

**Figure 3.1-8.** Topo pair for a  $\text{Fe}^{3+}/\text{Cu}^+$  galvanic cell. Upper surface  $\text{Fe}^{3+}/\text{Fe}^{2+}$ : yellow reduction path shows  $\text{Fe}^{3+} + \text{e}^- \rightleftharpoons \text{Fe}^{2+}$  with a starting point of  $\text{Fe}^{3+}$  at unit activity and  $\text{Fe}^{2+}$  essentially absent. Lower surface  $\text{Cu}^{2+}/\text{Cu}^+$ : red oxidation path shows  $\text{Cu}^+ \rightleftharpoons \text{Cu}^{2+} + \text{e}^-$  with a starting point of  $\text{Cu}^+$  at unit activity and  $\text{Cu}^{2+}$  essentially absent.

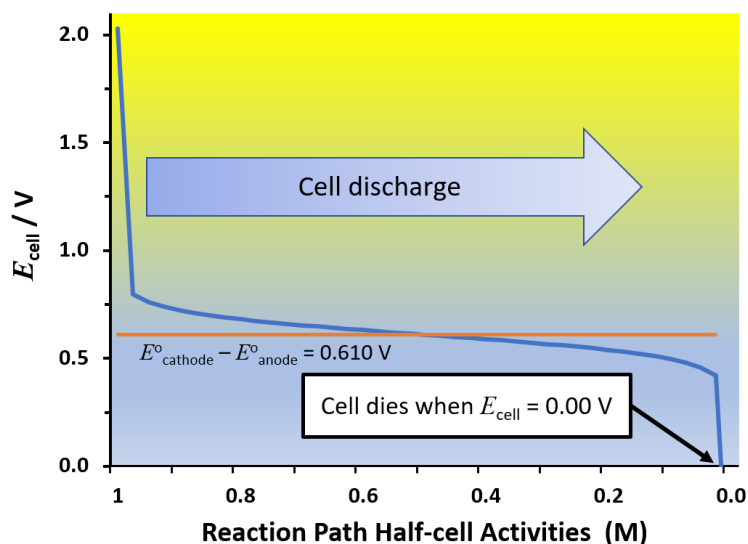


As the  $\text{Fe}^{3+}$  is consumed, the potential quickly drops from the left-hand bluff down onto the  $E^0$  plateau area for the  $\text{Fe}^{3+}/\text{Fe}^{2+}$  couple. The  $\text{Fe}^{3+}$  reduction reaction continues to be spontaneous as long as the reaction path potential is greater than that in the Cu half-cell. As can be seen in the figure, the entire  $E^0$  plateau for  $\text{Fe}^{3+}/\text{Fe}^{2+}$  is well above the  $E^0$  plateau for  $\text{Cu}^{2+}/\text{Cu}^+$ . The reaction path moves diagonally across the surface until it hits the front cliff. As the  $\text{Fe}^{3+}$  is nearly depleted, the potential quickly plummets. At the same time, the  $\text{Cu}^+$  oxidation path runs in the opposite direction on the lower surface. It rises rapidly from its start low on the front cliff, progresses diagonally across the  $E^0$  plateau for  $\text{Cu}^{2+}/\text{Cu}^+$  to its left-hand bluff, and then begins to rapidly climb as the  $\text{Cu}^+$  is nearly depleted. Because both half-cell reactions involve a one  $\text{e}^-$  transfer and all species in the cell's overall chemical equation have a coefficient of one, this is a stoichiometrically symmetric reaction. Thus, the  $\text{Fe}^{3+}$  is nearly depleted at the same time as the  $\text{Cu}^+$  is nearly depleted. The galvanic cell reaction stops when the dropping  $\text{Fe}^{3+}$  path and the rising  $\text{Cu}^+$  path achieve the same potential. Given the symmetry, this is a point exactly half-way between the two  $E^0$  plateaus. (Note: This is an ideal simulation system. To set up this sample case in the real world, concentrations would need adjustments to make the activity of the two reactants

equal. The activity effect on  $\text{Fe}^{3+}$  would be more pronounced because of its higher charge than  $\text{Cu}^+$ .  $\text{Fe}^{3+}$  would need to be at a higher concentration. For example, at an ionic strength ( $\mu$ ) of 0.1 M, the activity coefficient for  $\text{Fe}^{3+}$  is 0.18 while that for  $\text{Cu}^+$  is 0.405. Thus, a solution with  $\mu = 0.1$  would require a concentration of  $\text{Fe}^{3+}$  that was 2.25 times that of  $\text{Cu}^+$  for the two to be at the same activity.)

Note that most of the discharge paths for both half-cells track across their relatively flat  $E^0$  plateaus. This results in a fairly constant voltage for the cell (Figure 3.1-9). In this case,  $E_{\text{cell}}$  will quickly establish itself near  $E^0_{\text{cathode}} - E^0_{\text{anode}} = 0.771 \text{ V} - 0.161 \text{ V} = 0.610 \text{ V}$ . This near constant voltage will be continuously delivered until both  $\text{Fe}^{3+}$  and  $\text{Cu}^+$  are nearly depleted when both of the symmetric paths near the edge of their plateau regions. Then, in short order, the “battery” will quickly die, as detailed in the next chapter. Of course, in the real world, cell potentials would not be those that are idealized here because of other circuit contributions such as electrode junction potentials, diffusion potentials and IR drop.

**Figure 3.1-9.** Cell potentials during discharge for the  $\text{Fe}^{3+}/\text{Cu}^+$  galvanic cell of Figure 3.1-8.



The “Galvanic cell reaction paths” tab of the Redox TOPOS software will automatically determine the reaction paths as a cell discharges to a 0.00 V dead point. The user simply inputs the information for the two half-cells involved: the two  $E^0$ s, the starting activities for the oxidized and reduced forms of the two redox couples, and stoichiometric coefficients from the two half-cell reactions, including the number of electrons. Redox TOPOS then searches for the point on

each half-cell's Nernst surface that yields an overall  $E_{\text{cell}} = 0.00 \text{ V}$ . For the symmetric pair of half-cell reactions in Figure 3.1-8,  $E_{\text{cell}} = 0.00 \text{ V}$  halfway between the two  $E^0$  values,  $E_{\text{Fe path}} = E_{\text{Cu path}} = (0.771 \text{ V} + 0.161 \text{ V})/2 = 0.466 \text{ V}$ . This voltage is displayed in the red "Cell Discharge Progress" textbox (Figure 3.1-10). When this  $\text{Fe}^{3+}/\text{Cu}^+$  system is run, both half reactions display  $E_{\text{anode}}$  and  $E_{\text{cathode}}$  values of 0.466 V at the final point. Notice, too, that both reactive species are essentially depleted ( $7 \times 10^{-6} \text{ M}$ ) while both product species are essentially equal to 1.0 M. The reaction paths in Redox TOPOS are plotted on a pair of 2-D composition grids. Excel is not capable of drawing a reaction path superimposed on the 3-D Nernst surface plots. With care, however, they can be added manually by using Excel's drawing tools, as was done to generate Figure 3.1-8.

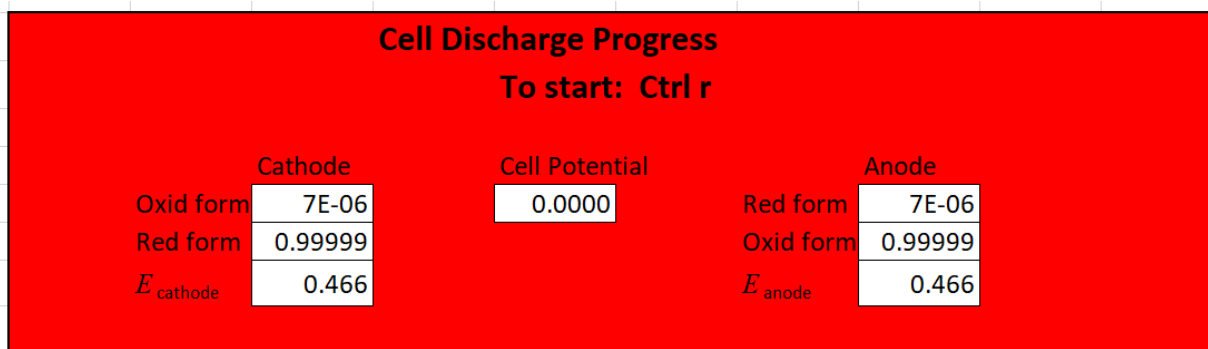


**Figure 3.1-10.** The Cell Discharge Progress textbox from running Redox TOPOS when the galvanic cell reaction for the  $\text{Fe}^{3+}/\text{Cu}^+$  galvanic cell of Figure 3.1-8 is used as input. The cathode reaction is reduction of  $\text{Fe}^{3+}$ ; the anode reaction is oxidation of  $\text{Cu}^+$ .

### 3.1.6 Concentration Cells

The Nernst surface approach nicely illustrates how concentration cells work, too. As noted earlier, this is the cell type which Nernst originally characterized. A concentration cell is simply a galvanic cell in which both electrodes are identical and the electrolytes in the two half-cells are the same except in concentration. Only one Nernst surface is needed here to represent the cell discharge process. The driving force for a concentration cell comes from choosing a pair of starting coordinates on the redox grid that have substantially different potentials. This generally means one half-cell will be enriched in the

oxidized form of the couple (high, toward the left-hand bluff) and the other half-cell predominantly holds the reduced form (low, toward the front cliff).

Consider, for example, a concentration cell comprised of two  $\text{Fe}^{3+}/\text{Fe}^{2+}$  half-cells. In the cathode half-cell, assume that  $\text{Fe}^{3+}$  is present at 1.0 M activity while there is essentially no  $\text{Fe}^{2+}$  (*i.e.*,  $1.0 \times 10^{-24}$  M). The anode half-cell contains exactly the opposite composition, the  $\text{Fe}^{2+}$  activity of 1.0 M and the  $\text{Fe}^{3+}$  is set at  $1.0 \times 10^{-24}$  M. Because of the symmetry selected for this case, the two reaction paths will collide head-on in the exact center of the  $E^0$  plateau. As this central point is on the diagonal between the origin at (0.0,0.0) and the  $E^0$ -defining point at (1.0,1.0), the concentration cell will die when both  $E_{\text{cathode}}$  and  $E_{\text{anode}}$  are equal to the  $E^0$  value of 0.771 V (Figure 3.1-11). Both discharge paths are on the same  $E^0$  plateau, meaning that their  $E_{\text{half-cell}}$  values are relatively close in magnitude. Voltages from concentration cells are small. Concentration cells are useful more as a standard reference potential, than to deliver a current as a battery.

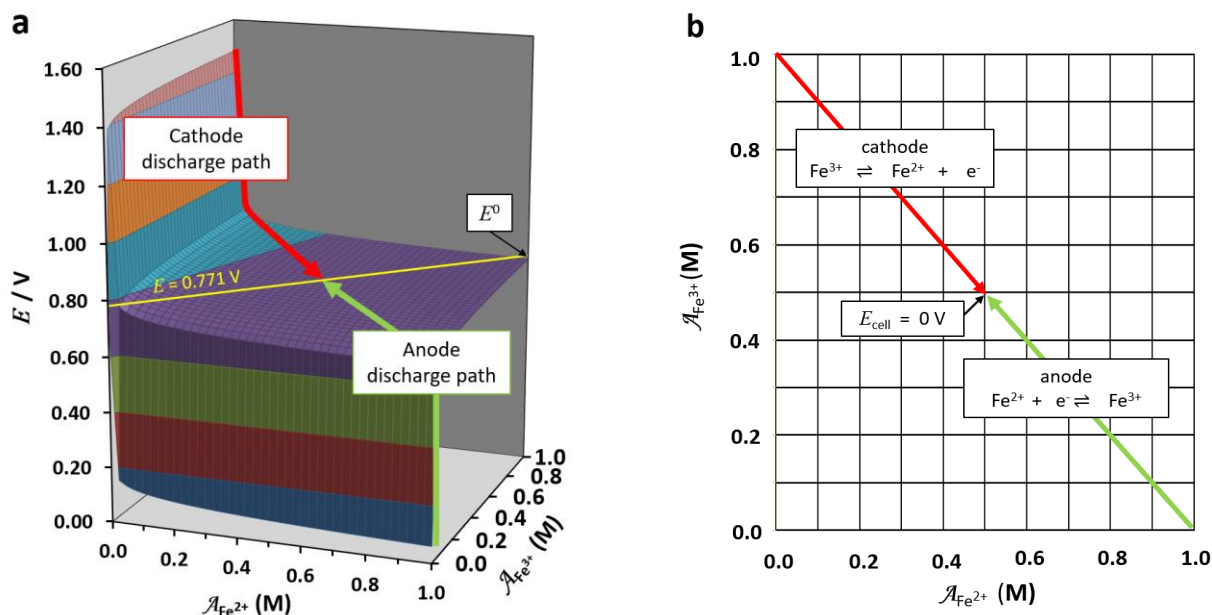


**Figure 3.1-11.** A sample  $\text{Fe}^{3+}/\text{Fe}^{2+}$  concentration cell. The cathode half-cell starts at essentially all  $\text{Fe}^{3+}$ ; the anode half-cell at essentially all  $\text{Fe}^{2+}$ . The two discharge paths meet at the surface diagonal where  $E_{\text{cathode}} = E_{\text{anode}} = 0.771$  V (equivalent to  $E^0$ ). a) Nernst topo; b) composition grid.

### 3.1.7 Varying Adjustment Term Parameters

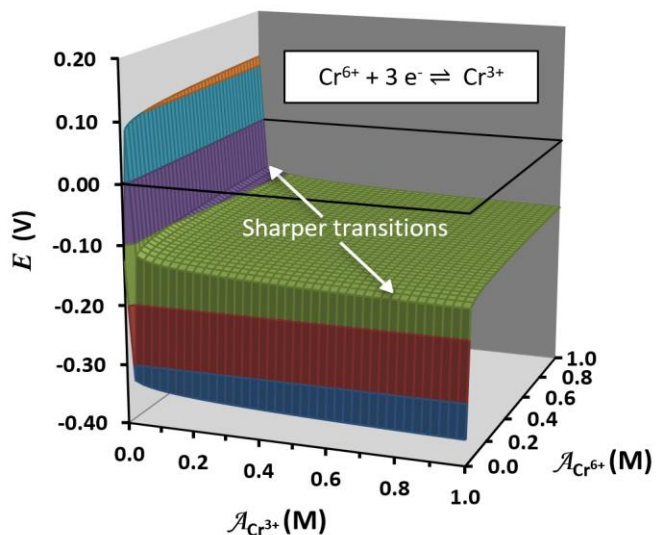
The adjustment term of the Nernst equation (see Figure 3.1-3)

$$\frac{RT}{nF} \ln \frac{\mathcal{A}_{\text{ox}}^a}{\mathcal{A}_{\text{red}}^b}$$

includes a number of parameters that can affect the overall look of the resultant topo surface. These include  $n$  (the number of electrons transferred) and  $T$  (the temperature in kelvin). Additional changes in the right-hand quotient can include pH (if hydronium or hydroxide ions are present in a half-reaction) and disappearance of the oxidized or reduced form when it is a solid or pure phase. This section details the changes imparted to the Nernst surface as various parameters undergo change.

The number of electrons transferred in the half reaction,  $n$ , appears in the denominator of the adjustment term's coefficient. Its effect on linear surfaces is to alter the slope of the plateau. This is particularly noticeable where the plateau rises up against the left-hand bluff or drops off of the front cliff. The higher the  $n$ -value, the flatter the plateau is as it approaches the left and front edges. Figure 3.1-12 presents the surface for the three-electron transfer  $\text{Cr}^{6+} + 3\text{e}^- \rightleftharpoons \text{Cr}^{3+}$  with  $E^0 = -0.12\text{ V}$  (in 1 F NaOH). The transitions to the left-hand wall and front face are slightly more angular compared to the single-electron half-reactions illustrated in previous topos.

**Figure 3.1-12.** The Nernst surface for the  $3\text{e}^-$  transfer in the  $\text{Cr}^{6+}/\text{Cr}^{3+}$  half-cell.

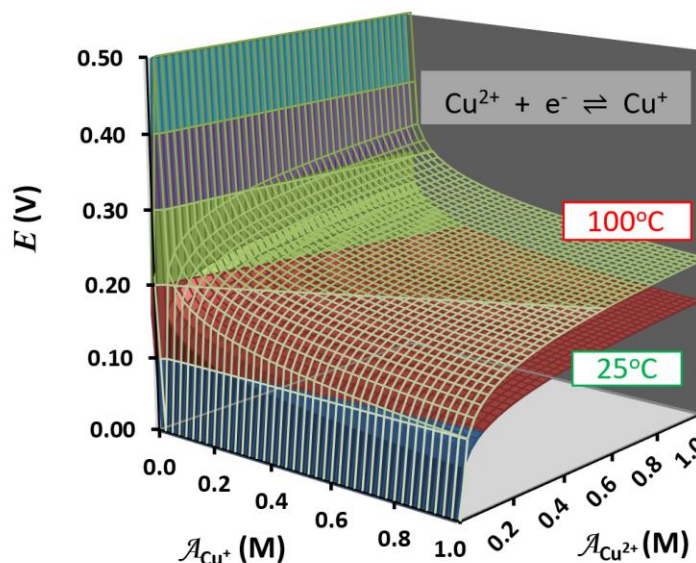


Changing the temperature of a half-cell has two effects with respect to the Nernst surface. First,  $E^0$  itself is a function of temperature, so the  $E^0$  used for the surface must be corrected. Second, the appearance of  $T$  in the numerator of the adjustment term's coefficient imparts a slight increase in the slope of the plateau portion of the surface. Both of these effects can be seen for the  $\text{Cu}^{2+}/\text{Cu}^+$  couple in Figure 3.1-13. An upper limit of  $100^\circ\text{C}$  was selected to accentuate the maximum effect of temperature changes that are available in an aqueous medium. The  $E^0$  was corrected from its value of  $0.161\text{ V}$  at  $25^\circ\text{C}$  to  $0.219\text{ V}$  at  $100^\circ\text{C}$  using the relationship<sup>6</sup>

$$E^0(T) = E^0 + (dE^0/dT)\Delta T \quad (3.1-5)$$

Because the  $E^0$  at  $100^\circ\text{C}$  is larger, the entire surface is displaced upward by the standard potential term of the Nernst equation. The overall effect, however, is fairly small, only  $0.0582\text{ V}$  in this case. The  $z$ -axis of Figure 3.1-13 was expanded to accentuate the difference.

**Figure 3.1-13.** Nernst surface for the  $\text{Cu}^{2+}/\text{Cu}^+$  half-cell at two temperatures showing the upward offset and increased slope at the higher temperature.



Many half-reactions include species that can undergo changes in activity other than the actual redox couple itself. The most common additional species are hydronium ion,  $\text{H}_3\text{O}^+$ , or hydroxide ion,  $\text{OH}^-$ . Their activities appear as extra factors in the logarithmic portion of the adjustment term, products in the

numerator and reactants in the denominator. Consider, as an example, the reduction half-reaction

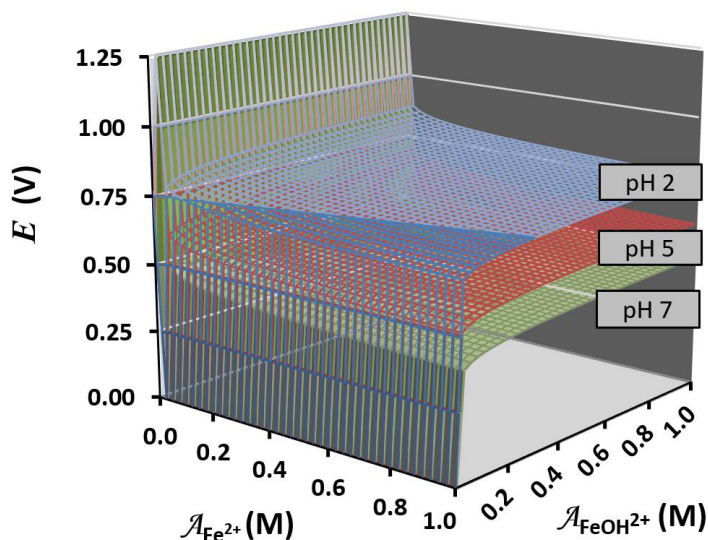


At fixed pH, the adjustment term for this reaction at 25°C is:

$$0.05917 \log \frac{\mathcal{A}_{\text{FeOH}^{2+}} \mathcal{A}_{\text{H}_3\text{O}^+}}{\mathcal{A}_{\text{Fe}^{2+}}} = 0.05917 \log \mathcal{A}_{\text{H}_3\text{O}^+} + 0.05917 \log \frac{\mathcal{A}_{\text{FeOH}^{2+}}}{\mathcal{A}_{\text{Fe}^{2+}}} \quad (3.1-7)$$

The first term on the right-hand side is the offset of the entire surface from the  $E^0$  value. The lower the pH, the higher the activity of  $\text{H}_3\text{O}^+$  and the bigger the offset. This is easily seen in Figure 3.1-14 where the topos for pH = 2.0 (upper surface), pH = 5.0 (middle surface) and pH = 7.0 (lower surface) are superimposed on the same axes. The surfaces are identical except for the added constant offset. These offsets result in a plateau elevation that is often quite removed from the  $E^0$  value as in simpler systems. In an experimental setting for which pH is not fixed, the potential would change 0.05917 V for each pH-unit shift that the half-cell solution experiences. An additional complication would be the shift in complex ion activities, *i.e.*, alpha coefficients for fractional composition diagrams, occasioned by any hydrolytic ligand interactions of the redox couple species.

**Figure 3.1-14.** Nernst topos for the  $\text{Fe}(\text{OH})^{2+}/\text{Fe}^{2+}$  half-reaction at three pHs.



Finally, Nernst surfaces for cell reactions with a redox couple species that is a solid or a pure liquid phase look different from those already discussed. They will simply be missing the left-hand bluff or the front cliff depending on which species comprises the pure phase. The activity for a pure phase is always defined as unity. Figure 3.1-15 shows an example of each. The upper surface is for a half-cell with a solid reduced form.

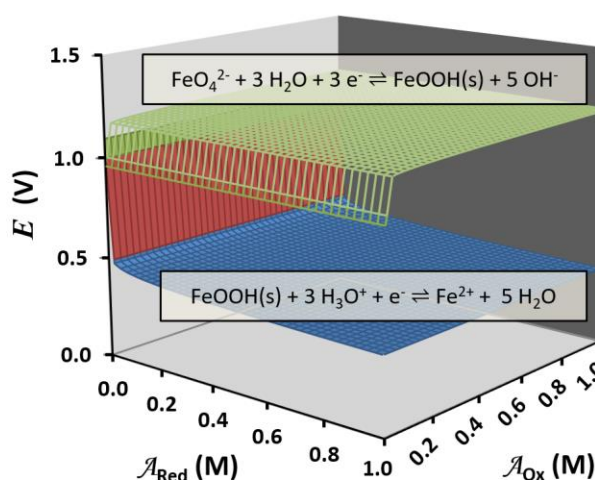


Because its Nernst equation has an activity term equal to 1 in the denominator of the logarithm factor, it never increases toward  $+\infty$  to form the left-hand bluff feature. While pure phase surfaces carry no new information on the pure phase axis, they are still useful to view when interacting with other half cells that have both left-hand bluffs and front cliffs. The  $x$ -axis for this surface should read 1.0 M for every slice, but we retain the same axis arrangement for comparative purposes. In a similar fashion, the lower surface of Figure 3.1-15 relates to a half-cell with a solid oxidized form.



The Nernst equation for this half-reaction has an activity term in the numerator of the logarithm factor equal to 1. The ratio of species never goes to zero and its logarithm never plummets to  $-\infty$  to form the front cliff. For this surface, the  $y$ -axis should read 1.0 M for each tick mark.

**Figure 3.1-15.** Two Nernst surfaces for half reactions with a solid phase redox couple species. Upper surface – solid product; lower surface – solid reactant.



### 3.1.8 Conclusions

This chapter introduces a composition grid designed to illustrate the behavior of the Nernst equation over a wide range of conditions for redox couples. It is especially helpful in

- visualizing the behavior of the Nernst equation over a wide range of conditions, not just a single solution composition as is the typical practice;
- dramatically illustrating via its broad plateaus that the potential for a given redox couple is usually close to its  $E^0$  value unless one or the other form of the couple is nearly depleted;
- identifying the single set of conditions that correspond to the definition of  $E^0$ , yet indicating that there is always a locus of other compositions on the surface that share the same voltage as  $E^0$ , a straight line when the coefficients of both forms are the same and a curved line when they are not;
- displaying reaction paths that represent the sequence of potentials that a half-cell moves through as the half-reaction proceeds, irrespective of whether it is part of an electrochemical cell or not;
- demonstrating, as a vertical separation between two Nernst surfaces, the potential difference that powers a galvanic cell when it undergoes discharge; and
- providing an image of the conditions under which a galvanic cell “dies”, *i.e.*, when the half-cell potential for both the anode and the cathode are equal and yield an  $E_{\text{cell}} = 0$ ;

The Redox TOPOS software is easy to run. Sliders allow the user to select the half-reaction's  $E^0$ ,  $n$  or  $T$  from which to compute the surface. Users must insert stoichiometric parameters for the oxidized and reduced forms of a half-reaction in the “Coefficients” input box. Other user-controlled variables can include  $\text{H}_3\text{O}^+$  or  $\text{OH}^-$  species (with the pH specified) and pure phases (solids or

liquids). Use of Redox TOPOS is appropriate for introductory courses when they are addressing the Nernst equation. The interpretation of some modeling results, however, will require the chemical sophistication of students in junior- or graduate-level courses in analytical chemistry, physical chemistry, biochemistry and aquatic chemistry. The speed and ease with which new systems can be visualized makes this a powerful tool for simulation studies.

Because Redox TOPOS is implemented via Microsoft Excel, no new software need be purchased to run it. Slider changes in Nernst equation variables result in near real-time alterations to the associated topos, with a second of releasing the mouse. On a separate tab, experimental paths are calculated by an iterative macro with run-times usually less than 20 seconds. Redox TOPOS can conveniently be used for “on the fly” calculations by an instructor during a live classroom session. A query from a student about “What would happen to the Nernst surface if...” can quickly be addressed with a new change in parameters or a run of the reaction path program.

### 3.1.9 Supplementary files

Five downloadable files are included as additional supplements for this chapter:

1. The downloadable Redox TOPOS software implemented as a Microsoft Excel workbook that includes possible redox couples and their associated  $E^0$  values. Users can supply their own information for systems not included in the compilation. The software automatically corrects  $E^0$  values for temperature changes if a  $dE^0/dT$  value is included.
2. A set of Microsoft PowerPoint slides from which to present a lecture on 3-D Nernst surfaces. Teaching points are highlighted and illustrated with extensively annotated surfaces.
3. The “Teaching with Redox TOPOS” file contains itemized learning objectives, with each objective matched to a range of slides in the PowerPoint file. Also included are suggested Redox TOPOS workbook activities (homework, prelab, recitation, or peer-led team discussions).

4. A detailed explanation of how the macro generates reaction paths for the cathode and the anode during a galvanic cell discharge.
5. A code listing for the galvanic cell discharge macro.

## Author Information

### Corresponding Author

\*E-mail: [garon.smith@umontana.edu](mailto:garon.smith@umontana.edu)

### ORCID

Garon C. Smith: 0000-0003-0145-8286

## Acknowledgments

The authors are grateful to the Department of Chemistry and Biochemistry at the University of Montana for graduate teaching assistantships during the doctoral program of MMH. The project was partially supported by a grant from North South University, Bangladesh Award No. NSU-RP-18-026. Portions of this manuscript were completed during a writing retreat at the University of Washington's Helen Riaboff Whiteley Center on San Juan Island, USA. Patrick MacCarthy, Department of Chemistry and Geochemistry, Colorado School of Mines contributed to early formulation of the redox composition grid concept.

## References

1. Allakhverdiev, S. I.; Tomo, T.; Shimada, Y.; Kindo, H.; Nagao, R.; Klimov, V. V.; Mimuro, M. Redox potential of pheophytin *a* in photosystem II of two cyanobacteria having the different special pair chlorophylls. *Proc. Natl. Acad. Sci. USA*, **2010**, *107*(8), 39243929.  
<https://doi.org/10.1073/pnas.0913460107>
2. Yan, F.; Ozsoz, M.; Sadik, O.A. Electrochemical and conformational studies of microcystin-LR. *Anal. Chim. Acta*, **2000**, *409*, 247–255.  
[https://doi.org/10.1016/S0003-2670\(99\)00888-0](https://doi.org/10.1016/S0003-2670(99)00888-0)

3. Shaposhnik, V. J. Walter Nernst and Analytical Chemistry. *J. Anal. Chem.*, **2008**, 63(2), 199-201.  
<https://doi.org/10.1134/S1061934808020160>
4. Nernst, W. Z. Die elektromotorische Wirksamkeit der Ionen. *Phys. Chem.* **1889**, 4, 129-181.  
<https://doi.org/10.1515/zpch-1889-0412>
5. Peters, R. Z. Ueber Oxydations- und Reduktionsketten und den Einfluss komplexer Ionen auf ihre elektromotorische Kraft. *Phys. Chem.* **1898**, 26, 193-236.  
<https://doi.org/10.1515/zpch-1898-2618>
6. Harris, D. *Quantitative Chemical Analysis*. 8<sup>th</sup> Edition; Freeman: New York, 2010, AP20-AP27. ISBN: 1429218150
7. de Levie, R. Redox Buffer Strength. *J. Chem. Educ.*, **1999**, 76 (4), 574-577.  
<https://doi.org/10.1021/ed076p574>